

CURRENT AND FUTURE TRENDS IN MEDICAL IMAGING AND IMAGE ANALYSIS

Recent advances in medical imaging modalities have laid the foundation for developing new methodologies to meet critical challenges in diagnostic radiology, treatment evaluation, and intervention protocols. The wide spectrum of multidisciplinary technologies that are being developed today and will continue in the future provides a better understanding of human physiology and critical diseases such as neurological disorders including Alzheimer's and Parkinson's.

14.1. MULTIPARAMETER MEDICAL IMAGING AND ANALYSIS

As described in Chapters 4–7, medical imaging modalities offer complementary information for the understanding of physiology and pathologies from molecular to organ levels. Current and future trends in functional magnetic resonance (fMR), diffusion MR, positron emission tomography (PET), ultrasound, and optical imaging are targeted toward obtaining molecular information from the cellular structure of tissue.

Future technological developments in multimodal molecular and cellular imaging should allow early detection of cellular/neurological deviations in critical diseases such as Alzheimer's, autism, or multiple sclerosis, before the first symptomatic signs. This is of great importance for better health care and prognosis. Current imaging paradigms rely on the expression of the first symptomatic signs, and then try to correlate, on an ad hoc basis, the observed signs with cellular and/or neurological deviations. The problem is that by the time the symptoms are expressed, the disease is probably already in a relatively advanced stage. Therefore, it is important that future imaging protocols are able to detect critical diseases in a presymptomatic stage for early diagnosis, treatment, evaluation, and intervention protocols.

Multimodality imaging and image registration have provided researchers and clinicians with important tools in diagnostic radiology. Multiparameter measurements are essential for the understanding and characterization of physiological processes. However, a multiparameter-based imaging protocol must optimize the data acquisition methods to acquire and analyze anatomical, metabolic, functional, and molecular signatures. It is important to study the variability associated with the respective structures to develop models that would further help to improve the imaging and image analysis protocols. Thus, continuous technological developments put new knowledge back into the learning cycle.

A generic paradigm for model-based medical imaging and image analysis is shown in Figure 14.1. As the computing, biochemical, and bioinstrumentation technologies continue to develop, future imaging modalities would be able to measure more parameters with higher spatial and temporal resolution. The last two decades have been largely focused on establishing the foundation of MR, single photon emission computed tomography (SPECT), PET, and ultrasound imaging modalities. Sophisticated imaging methods including perfusion, diffusion, and fMR and neuroreceptor-based fast PET have been developed to acquire more information about the physiological metabolism under specific functions (1–4). As shown in Figure 14.1, appropriate models of generalized physiological structures, imaging agents, and tissue-specific biochemical responses must be used to optimize the imaging protocols for structural and functional imaging. The model-based selection criteria would thus provide important information about the imaging parameters that can be used in a programmable way to intelligently control the imaging instrumentation. Once the data are acquired, variability models in generalized anatomical and metabolic structures can be used to improve feature selection, analysis, and interpretation.

Recent advances in MR imaging (MRI), functional MRI (fMRI), perfusion MRI (pMRI), and diffusion MRI (diffusion weighted imaging [DWI]/diffusion tensor imaging [DTI]) have provided the ability to study the functional and physiological behavior of the brain, allowing measurement of changes in blood flow and oxygenation levels for tissue characterization. While PET provides useful metabolic and receptor-site (pathophysiological) information, it lacks the ability to define anatomical details. MRI, on the other hand, provides high-resolution anatomical and physiological information. To study the physiological and functional aspects of the brain and tissue characterization, it would clearly be useful to combine PET, MRI, fMRI, pMRI, and DTI as a part of the postprocessing registration or, if possible, through simultaneous imaging.

Postprocessing image registration methods, although having the advantage of analyzing data off-line for mapping, suffer from uncertainties and errors in localization studies. This is primarily due to the small volume of interest defined for localization, limitations on resolution with different modalities, and computational inaccuracies in the postprocessing methods. For a given subject, the localized volume of interest may be small for a specific activation signal and may require submillimeter resolution. In addition, analysis of small localized volumes of interest may be needed for cellular characterization in understanding their physiological responses. Thus, accurate coregistration of the spatially distributed signals from different

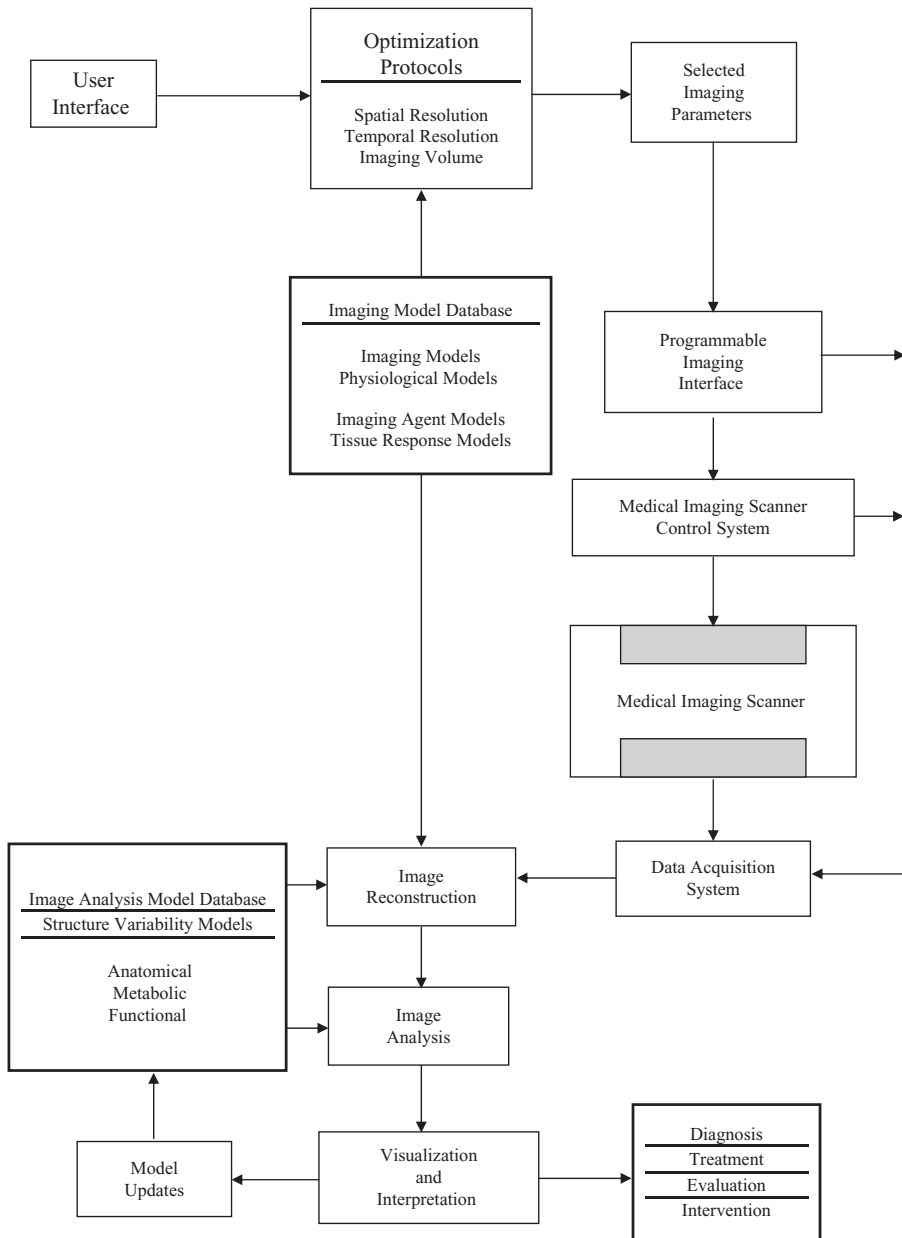
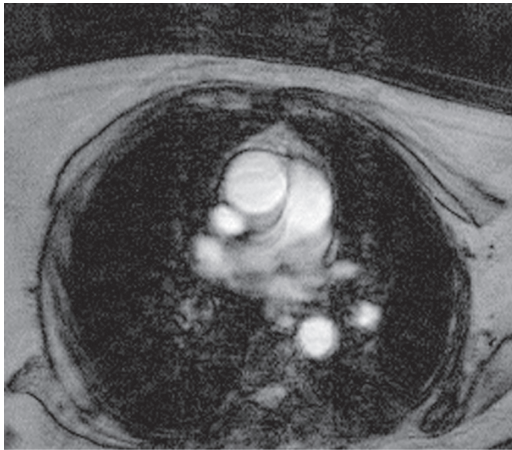


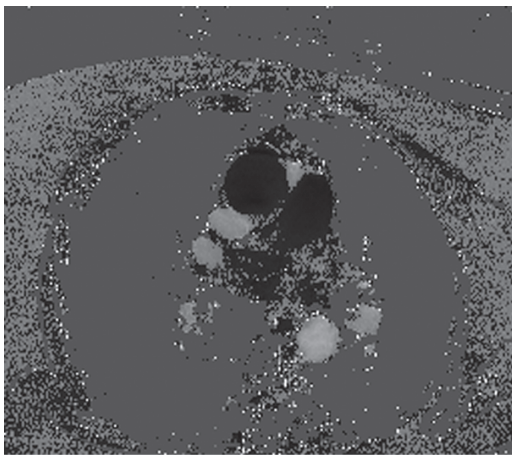
Figure 14.1 A multiparameter imaging and image analysis paradigm.

imaging modalities is an important requirement for studying physiological and functional behavior, specifically for neurological applications.

Current challenges in physiological and functional imaging include more robust and accurate imaging of cardiac motion, tissue-specific tumor imaging, and fast



(a)



(b)

Figure 14.2 (a) The velocity encoded MR magnitude and (b) phase image of the human cardiac cavity.

neuroreceptor tagging-based imaging of the brain for cortical functional imaging. These are just examples of the challenges in diagnostic radiology and are by no means a complete representation of a large number of issues in human physiology and pathology. Recently, MRI methods have been used with magnetization transfer, tissue tagging, and phase contrast encoding methods for acquiring cine images of the beating heart (5–7). Figure 14.2 shows images of cardiac cavity with velocity-encoded MRI magnitude (Fig. 14.2a) and phase (Fig. 14.2b) information. Figure 14.2a shows the magnitude image representing the anatomical structure. The areas with blood vessels appear bright because of the high water content. Figure 14.2b represents a velocity map, in which the medium gray corresponds to stationary tissue, the darker areas correspond to negative flow, and the brighter areas correspond to positive flow.

14.2. TARGETED IMAGING

Targeted molecular imaging methods can provide a systematic investigation into a physiological process for the assessment of a specific pathology. Recent discoveries in molecular sciences and imaging contrast agents have played a significant role in designing specific biomarkers to work with medical imaging modalities such as ultrasound, PET, fMR, and optical fluorescence imaging to study molecular responses linked with the onset of a disease. Contrast agents are used to image physiology or pathology that might otherwise be difficult to distinguish from the surrounding tissue. For example, encapsulated microbubbles in ultrasound imaging can provide information about activated neutrophil, a cell involved in the inflammatory response (<http://www.ImaRx.com>).

The technology for a specific contrast agent for targeted imaging can also be used for better drug delivery in critical therapeutic protocols. It is expected that future diagnostic, treatment-evaluation, and therapeutic-intervention protocols will use specific multimodality targeted imaging with computerized analyses through models using molecular signatures of physiological processes. For example, tumor-induced angiogenesis is a complex process involving tumor cells, blood, and the stroma of the host tissue. Studies related to angiogenic growth factors linked with endothelial cells have shown that vascular integrin $\alpha v \beta 3$ may be a useful therapeutic target for diseases characterized by neovascularization (8). Thus, $\alpha v \beta 3$ is a prime candidate for molecular targeting and can be monitored through advanced imaging methods. Furthermore, nanoparticle-conjugated novel MRI contrast agents can be used in order to directly observe gene expression, metabolism, and neurotransmission. The advantage of these novel contrast agents is their ability to provide such information in a noninvasive fashion. This enables important cellular and metabolic processes to be observed for the first time in whole animals over repeated time periods (9).

14.3. OPTICAL IMAGING AND OTHER EMERGING MODALITIES

Several imaging modalities have recently emerged that have a potential to play a significant role in diagnostic radiology. These modalities include optical, electrical impedance, and microwave imaging. Electrical impedance tomography (EIT) has been recently used for 3-D imaging of the breast (10–12). EIT methods of breast imaging have now begun to show promise in the noninvasive detection of tumors and circumscribed masses (12).

Optical imaging systems are relatively much less expensive, are portable, noninvasive, and adaptable to acquiring physiological and functional information from microscopic to macroscopic levels. For example, optical coherence tomography (OCT) is a noninvasive imaging technique capable of producing high-resolution cross-sectional images through inhomogeneous samples. It can offer a resolution level higher than current MRI, computed tomography (CT), SPECT, PET, and

ultrasound technologies. Although primary optical imaging modalities such as endoscopy have been used in clinical environments for several years, the clinical perspective of other advanced optical imaging modalities has yet to be established in diagnostic radiology. Recent advances in endoscopy, OCT, confocal microscopy, fluorescence imaging, and multispectral transillumination technologies show their great potential in becoming the mainstream diagnostic and treatment evaluation technologies of the future.

Optical imaging modalities may utilize the visible light spectrum from 400 to 700 nm of electromagnetic radiation to produce visible images in biomedical applications such as microscopy, endoscopy, and colonoscopy. However, the excitation and emission spectrum in advanced optical imaging modalities is not restricted to the visible spectrum but can be extended out on both sides into the soft ultraviolet ($<400\text{ nm}$) and near-infrared (NIR; $>700\text{ nm}$) ranges for fluorescence and multispectral imaging applications. The visible light spectrum, along with soft ultraviolet and NIR bands, follows relatively stochastic behavior in photon interaction and propagation in a heterogeneous multilayered biological tissue medium. Unlike X-ray photons, optical photons do not penetrate the entire biological tissue medium with predominantly straight transmission. Electromagnetic theories of light reflection, refraction, diffusion, interference, and propagation are described in depth by Born and Wolf (13) and are also discussed in recent books (14–16).

Light radiance is characterized by the total emission or reflection within a solid angle. It is the sum of all spectral radiances at individual wavelengths. As light passes through a heterogeneous multilayered medium, it suffers from wavelength-dependent absorption and scattering events. In a multilayered heterogeneous medium such as a biological tissue, characteristic absorption and scattering coefficients determine the light radiance at a given point. Light radiance is also described by the scattering phase function, which is defined as the cosine of the angle between the incident and scattered paths. The weighted average of the scattering phase function is called the anisotropy factor. In a biological tissue, the anisotropy factor is strongly peaked in the forward direction. However, a series of scattering events in a turbid medium with a continuously changing direction of light propagation can also produce backscattered diffused radiance, which can reemerge from the surface (17, 18). Figure 14.3 shows a schematic diagram of optical reflectance, backscattered diffused reflectance, and transmission imaging modalities in a multilayered biological tissue medium. For simplicity, each layer is assigned wavelength-dependent average absorption and scattering coefficients, an anisotropy factor, and an index of refraction.

14.3.1 Optical Microscopy

Microscopic imaging modalities provide a variable magnification and depth of field for imaging a tissue in an embedded medium or *in vivo*. The magnification power provides the capability to image the tissue at the cellular level. The distance at which an optical system can clearly focus is known as the depth of field. Within the depth of field, objects are in focus; that is, they appear crisp and sharp. At increasing distances outside the depth of field (either closer to or further away from

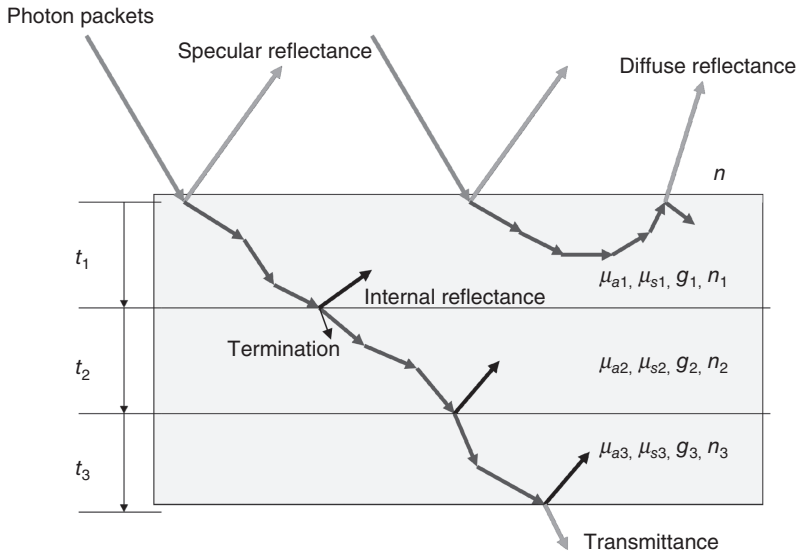


Figure 14.3 A simplified model of a biological medium with three layers. Each layer is associated with an absorption coefficient μ_a , a scattering coefficient μ_s , an anisotropic factor g , and a refractive index n .

the camera), objects gradually become more blurred. In typical photography, an image is comprised of the superposition of all the light originating from all depth planes, thus providing a wide field of view typical to what a human eye can see. For biological imaging, however, it is often desired to obtain separate images of individual depth planes. This is known as optical sectioning. In confocal microscopy, a small pinhole is used to block all out-of-focus light, therefore limiting the image to only the light reflected from objects in the focal plane. Multiphoton microscopy, on the other hand, is designed in such a way that light is emitted back only from the current point of interest. These techniques are often used to image the fluorescent light emitted from biological tissue on a slice-by-slice basis.

Fluorescence imaging uses ultraviolet light to excite fluorophores and then collect back emitted light at a higher wavelength. Fluorophores include endogenous and exogenous fluorophores. The former refers to natural fluorophores intrinsic inside tissue, such as amino acids and structural protein, and these fluorophores are typically randomly distributed. The latter usually refers to smart polymer nanoparticles targeting specific molecules such as hemoglobin. Because of its high resolution at the cellular and subcellular levels, as well as the ease of obtaining 3-D reconstructions, multiphoton microscopy is also often used for functional imaging, that is, the spatial and temporal visualization of biological processes in living cells (19). Two-photon microscopy has been applied to obtain a 3-D visualization over time of the accumulation and penetration of nanoscale drug vehicles within the skin (20), the cellular dynamics of immunology (21), mouse kidney development (22), as well as neuronal dendrite dynamics (23).

14.3.2 Optical Endoscopy

Endoscopy, as a medical tool for observation and diagnosis, is straightforward in concept and has existed since 1807 when Phillip Bozzini used candlelight and mirrors to observe the canals of the human body. Numerous developments through the decades since then have taken this technology through the initial introduction of electric light for internal illumination all the way to flexible endoscopes using fiber optics, gradually improving the quality, noninvasiveness, and impact of endoscopic procedures.

Applications of endoscopy within the body are wide-ranging, directed primarily in the upper and lower gastrointestinal tract such as the colon and esophagus, but also in areas such as the bladder and even the brain. In general, current research is focused on producing higher quality endoscopic images from smaller devices able to reach previously inaccessible locations inside the body. The primary goal is to improve early diagnostic capabilities, while reducing costs and minimizing patient discomfort. It is hoped that endoscopy may be able to provide an easy method for screening at-risk patients for signs of cancer or precancerous tissue, including dysplasia and neoplasia. It is difficult to detect dysplasia using conventional endoscopic techniques, such as white light endoscopy.

The gold standard of any endoscopic system is a histological analysis of a biopsied resection. Dysplasia can be detected through biopsy, but a suitable biopsy site needs to be selected. In addition to the typical detection of cancer and precancer in common endoscopic areas such as the upper and lower gastrointestinal tract, endoscopy has also found applications in a variety of other locations in the body, with a number of different imaging objectives. Endoscopic imaging of the brain, known as neuroendoscopy, is subjected to narrower restrictions, but still has promise to permit imaging of transventricular regions or to perform endoscope-assisted microsurgery (24, 25).

14.3.3 Optical Coherence Tomography

Optical coherence tomography was invented in early 1990s but has recently emerged as a popular 3-D imaging technology for biomedical applications (26–28). This relatively new modality makes use of the coherent properties of light. In an OCT system, light with a low coherence length is divided into two parts. One part serves as a reference while the other is directed into the tissue. When light travels in tissue, it encounters an interface with a different refractive index, and part of the light is reflected. This reflectance is subsequently mixed with the reference. Once the optical path length difference between the reference light and the reflected light is less than the coherence length, coherence occurs. By observing the coherence pattern and changing the optical path length of the reference light with a mirror, a cross-section of the tissue can be rendered. With a sufficiently low coherence length, the resolution of OCT may reach a magnitude on the micrometer scale; hence, it can disclose subtle changes in cancer tissue at the cellular level. OCT recovers the structure of interrogated tissue through a mechanism analogous to ultrasonic imaging. The latter

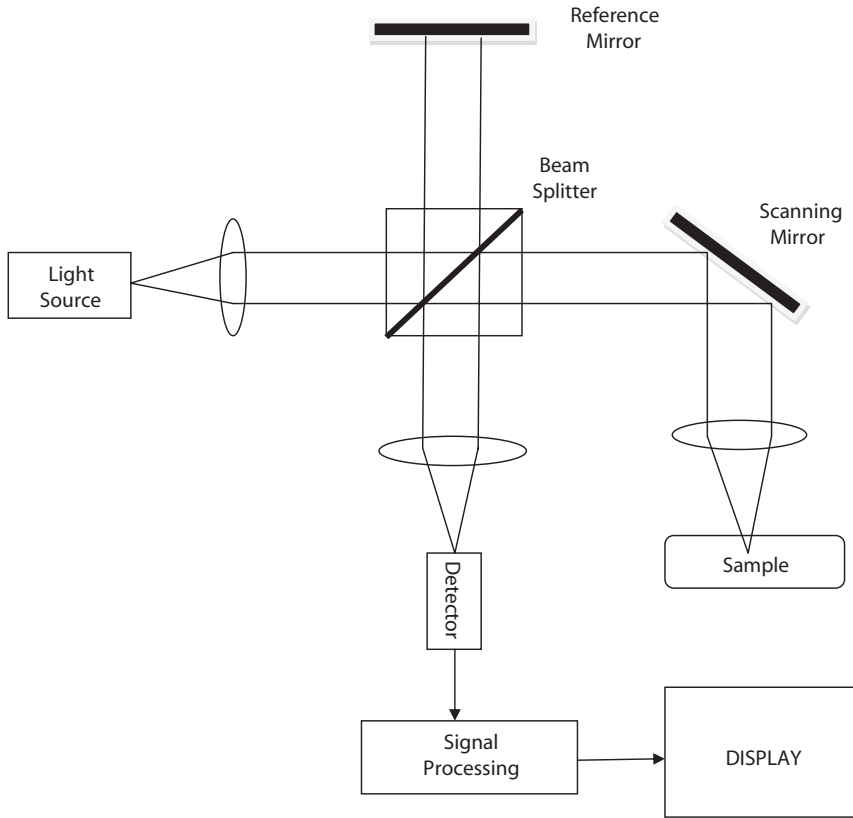


Figure 14.4 A schematic diagram of a single-point scanning-based optical coherence tomography system.

modality sends sound into tissue, which reflects when encountering an impedance-varied interface. The resolution of OCT is much higher than that of ultrasonic imaging, but it cannot penetrate as far.

There are two types of broadly classified OCT systems: a single-point scanning-based OCT system (Fig. 14.4) and a full-field OCT system (Fig. 14.5). Images can be produced in time domain OCT mode through low coherence interferometry in which the reference path length is translated longitudinally in time. A fringe pattern is obtained when the path difference lies within the coherence length of the source. In frequency domain OCT (FD-OCT), a broadband interference pattern is exploited in spectral dispersion. Spectrally separated detectors are encoded with optical frequency distribution onto a charge-coupled device (CCD) or CMOS detector array so that information about the full depth is obtained in a single shot. Alternatively, in time-encoded frequency domain OCT (TEFD-OCT, or swept source OCT), spectral dispersion on the detector is encoded in the time domain instead of with spatial separation (26–28).

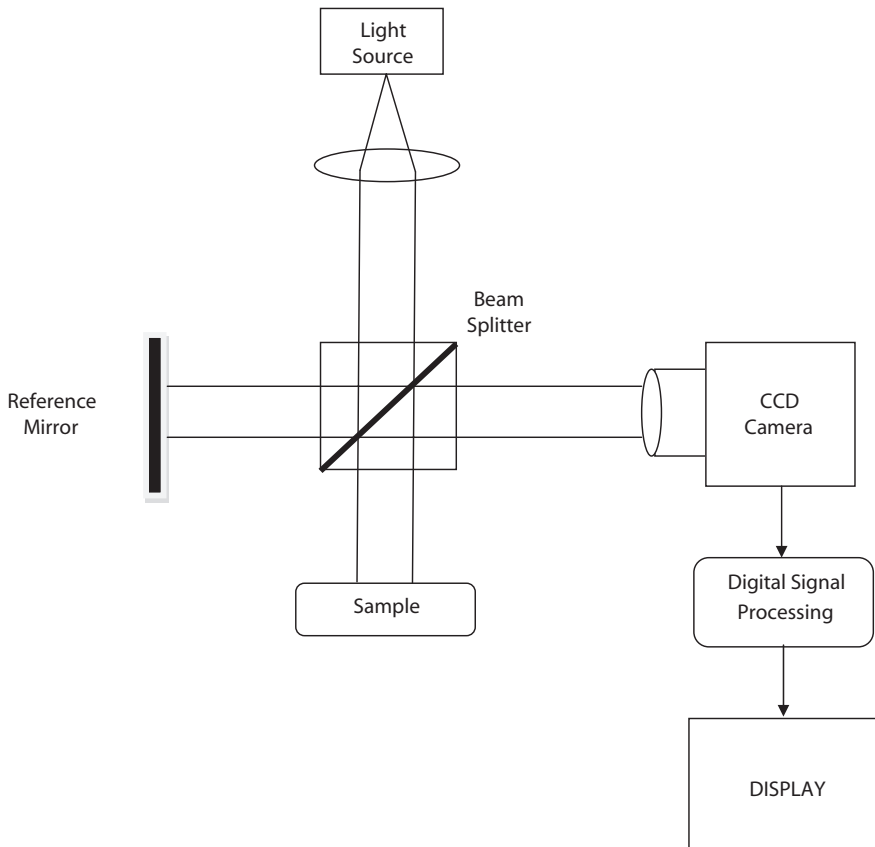


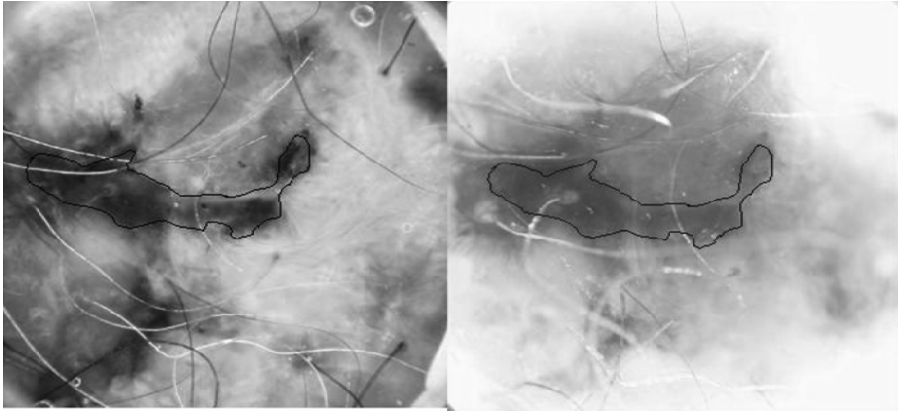
Figure 14.5 A schematic diagram of a full-field optical coherence tomography system.

14.3.4 Diffuse Reflectance and Transillumination Imaging

Diffuse reflectance images are formed by backscattered diffused light. These images represent composite information about the absorption and scattering by different chromospheres and biological structures in the medium. Although the raw images produced may be useful and may carry important diagnostic information, more significant information can be derived from the 3-D reconstruction of the biological medium from multispectral diffuse reflectance measurements.

Figure 14.6 shows a surface reflectance-based epi-illumination light microscopy (ELM) image (left) of a malignant melanoma skin lesion and a backscattered diffuse reflectance-based transillumination image (right) obtained by the Nevoscope (29, 30). Increased absorption due to greater blood volume around the outlined lesion's boundary is evident in the transillumination image (30).

Transillumination, also known as shadowgram optical imaging or diaphanography, was first used by Cutler in 1929 to examine pathology in the breast (31). Transillumination was initially surpassed by the superiority of X-ray technology but later evolved to be a major application of visible light in medicine, particularly in



Oil Epiluminescence

Transillumination

Figure 14.6 Surface reflectance based ELM image (left) of a malignant melanoma skin lesion with a backscattered diffuse reflectance-based transillumination image (right).

aiding the early detection and diagnosis of breast cancer. Because evaluating breast cancer risk assessment with optical transillumination would avoid the need for ionized radiation through X-ray mammography, it could be safely applied more frequently to women of all ages. The parenchymal tissue density pattern is a good indicator of future breast cancer risk, and is typically obtained through mammography. As an alternative, the chromophore composition and morphology of the breast tissue, as observed through transillumination, has been used to identify women with high parenchymal density. This method may therefore provide the same odds ratio for breast cancer risk as can traditional mammography; thus, it may offer an alternative to radiation screening (32–34).

While transillumination is often performed using white visible light, infrared and ultraviolet light are also commonly used to observe interesting tissue characteristics that may not be apparent under the visible spectrum. The recent widespread availability of NIR lasers and CCDs had led to further research in optical transillumination modalities with infrared light, particularly in the last two decades. Using an NIR laser (1250 nm) for transillumination, differences in contrast and resolution were observed between normal breast tissue and cancerous breast tissue (34).

14.3.5 Photoacoustic Imaging: An Emerging Technology

Photoacoustic imaging is a fast emerging technology that utilizes the acoustic waves from the thermal expansion of an absorbing object, such as a tumor, pigmented lesion, or blood vessel, caused by the absorption of light photons. In biomedical imaging applications, light from a short pulsed laser scatters inside the target object, producing heat. The temperature is raised by a fraction of a degree, causing thermal expansion. The thermoelastic effect generates pressure transients that exactly represent the absorbing structures. These pressure transients produce ultrasonic waves

that propagate to the tissue surface and are detected by an ultrasound sensor. The photoacoustic imaging methods are also known as optoacoustics, laser-induced ultrasound, or thermoacoustics imaging, and have been investigated for imaging lesions of the breast, skin, and vascular tissues. A nice overview of photoacoustic effect and imaging methods is presented in a dissertation by Niederhauser (35), and also in a tutorial paper by Wang (36). The spatial resolution of photoacoustic imaging depends on the photoacoustic emission phase. As described in (36), strong optical scattering in biological tissue causes shallow imaging depth and low spatial resolution. Because ultrasound scattering is much weaker than optical scattering, the resulting ultrasound signal from photoacoustic imaging provides better resolution than optical diffuse imaging methods for various medical imaging applications (36–40).

14.4. MODEL-BASED AND MULTISCALE ANALYSIS

The basic model-based methods for image reconstruction and analysis are described in Chapters 8–12. The trends of using more sophisticated multiparameter models in multidimensional medical image analysis will continue in the future. For example, probabilistic brain atlases incorporating specific anatomical and functional variability structures will continue to improve analysis, understanding, and visualization of brain images.

Figure 14.7 shows a visualization of cortical surfaces of a patient with a brain tumor (not shown in the image). The cortical activation due to tongue movement was measured with the fMRI and is superimposed on the cortical surface-rendered image. Figure 14.8 shows a 3-D surface-rendered image of the face and head with the cross-sectional volume visualization of MR data-based anatomical structures. The images shown in Figures 14.7 and 14.8 are just two of the many examples of multiparameter image analysis, registration, and visualization of human brain that have been explored for understanding pathologies as well as for image-guided surgery. There are still numerous challenges in this area to be addressed in the near future through the advances in multimodality multiparameter medical imaging and image analysis.

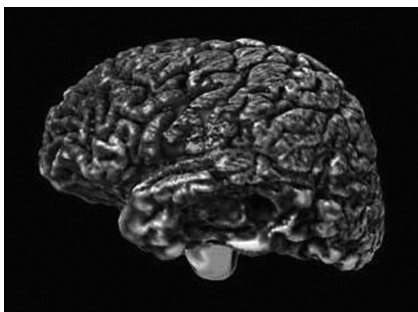


Figure 14.7 A surface visualization of cortical structure with the superposition of activation function (<http://www.bic.mni.mcgill.ca/>).

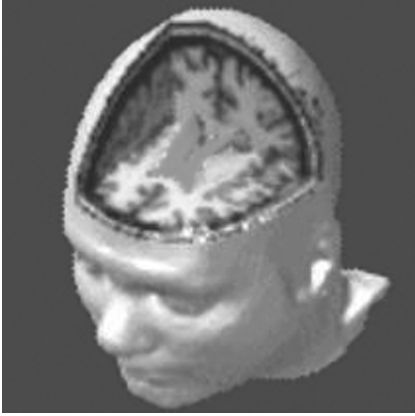


Figure 14.8 A surface visualization of human face with the volume visualization of anatomical structure of the brain (<http://www.bic.mni.mcgill.ca/>).

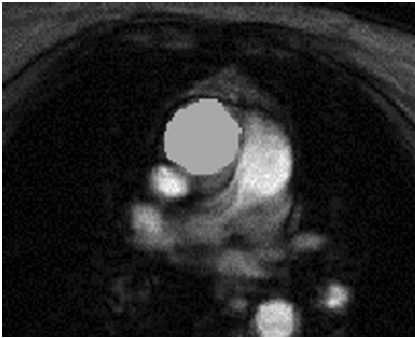


Figure 14.9 The segmentation of blood vessel shown in the magnitude and phase MR images of human cardiac cavity shown in Figure 14.2 using the wavelet-based frequency localization features.

Multiresolution-based wavelet processing methods have been used for several applications with significant improvements in tissue segmentation and characterization (41–44). Figure 14.9 shows the segmentation of a main blood vessel using wavelet processing on the magnitude and phase images shown in Figure 14.2. A training set of images was used for manual segmentation by experts to develop a signature model of the blood vessel using the wavelet processing-based frequency-localized features. Using the signature model with the nearest neighbor classifier, the blood vessel was segmented as shown in Figure 14.9.

In addition to multiparameter multiresolution image analysis, the advantage of complementary medical imaging modalities can also be realized through multiscale imaging from cellular to tissue and organ levels. For example, while optical imaging modalities such as fluorescence microscopy and OCT can provide information at the cellular level, X-ray CT, ultrasound, MRI, fMRI, and SPECT-PET imaging modalities can provide structural and functional information at tissue

and organ levels. Such multiscale analysis has been of significant interest and will continue in the future as an area of active research, specifically in neuroscience.

One of the major challenges in using multimodality multidimensional signal and imaging technologies for diagnostic and surgical applications is how to integrate information from different technological instruments. The process of information fusion requires computer processing of large data files with a common standard coordinate system so that information from different instruments can be easily read and integrated toward analysis of target areas. Large information processing, archiving, and retrieval systems such as Picture Archiving and Communication Systems (PACS) have been developed in radiological environment (45–47). Although efforts have been made in establishing common formats such as DICOM for different imaging scanners, it is a significant and challenging task to provide real-time fusion of multimodality signal and image processing features and correlate it to patient information for relevant information extraction that can be used for therapeutic and surgical intervention.

14.5. REFERENCES

1. S.L. Hartmann and R.L. Galloway, "Depth buffer targeting for spatial accurate 3-D visualization of medical image," *IEEE Trans. Med. Imaging*, Vol. 19, pp. 1024–1031, 2000.
2. M. Ferrant, A. Nabavi, B. Macq, F.A. Jolsez, R. Kikinis, and S.K. Warfield, "Registration of 3-D intraoperative MR images of the brain using a finite element biomechanical model," *IEEE Trans. Med. Imaging*, Vol. 20, pp. 1384–1297, 2001.
3. K. Rohr, H.S. Stiehl, R. Sprengel, T.M. Buzug, J. Wesse, and M.H. Kahn, "Landmark based elastic registration using approximating thin-plate splines," *IEEE Trans. Med. Imaging*, Vol. 20, pp. 526–534, 2001.
4. G.E. Christensen and H.J. Johnson, "Consistent image registration," *IEEE Trans. Med. Imaging*, Vol. 20, pp. 568–582, 2001.
5. J. Park, A.A. Young, and L. Axel, "Deformable models with parameter functions for cardiac motion analysis from tagged MRI data," *IEEE Trans. Med. Imaging*, Vol. 15, pp. 278–289, 1996.
6. G.J. Parker, H.A. Haroon, et al., "A framework for a streamline-based probabilistic index of connectivity (PICO) using a structural interpretation of MRI diffusion measurements," *J. Magn. Reson. Imaging*, Vol. 18, No. 2, pp. 242–254, 2003.
7. C.J. Baker, M.J. Hartkamp, and W.P. Mali, "Measuring blood flow by nontriggered 2D phase-contrast cine magnetic resonance imaging," *Magn. Reson. Imaging*, Vol. 14, pp. 609–614, 1996.
8. P.C. Brooks, R.A. Clark, and D.A. Cheresh, "Requirement of vascular integrin $\alpha_v\beta_3$ for angiogenesis," *Science*, Vol. 264, No. 5158, pp. 569–571, 1994.
9. T. Atanasićević, M. Shusteff, P. Fam, and A. Jasanoff, "Calcium-sensitive MRI contrast agents based on superparamagnetic iron oxide nanoparticles and calmodulin," *Proc. Natl. Acad. Sci. USA*, Vol. 103, pp. 14707–14712, 2006.
10. J. Jossinet, E. Marry, and A. Montalibet, "Electrical impedance endo-tomography: Imaging tissue from inside," *IEEE Trans. Med. Imaging*, Vol. 21, pp. 560–565, 2002.
11. T.E. Kerner, K.D. Paulsen, A. Hartov, S.K. Soho, and S.P. Poplack, "Electrical impedance spectroscopy of the breast: Clinical imaging results in 26 subjects," *IEEE Trans. Med. Imaging*, Vol. 21, pp. 638–645, 2002.
12. A.Y. Karpov, A.V. Korjenskij, V.N. Kornienko, Y.S. Kultiasov, M.B. Ochapkin, O.V. Trochanova, and J.D. Meister, "Three-dimensional EIT imaging of breast tissues: System design and clinical testing," *IEEE Trans. Med. Imaging*, Vol. 21, pp. 662–667, 2002.
13. M. Born and E. Wolf, *Principles of Optics: Electromagnetic Theory of Propagation, Interference and Diffraction of Light*, 7th Edition, Cambridge University Press, Cambridge, UK, 1999.

14. L.V. Wang and H.-I. Wu, *Biomedical Optics: Principles and Imaging*, John Wiley & Sons, Inc, Hoboken, NJ, 2007.
15. C. Bohren and D. Huffman, *Absorption and Scattering of Light by Small Particles*, Wiley-Interscience, New York, 1983.
16. A. Ishimaru, *Wave Propagation and Scattering in Random Media*, IEEE Press, New York, 1999.
17. A.N. Bashkatov, E.A. Genina, V.I. Kochubey et al., "Optical properties of human skin, subcutaneous and mucous tissues in the wavelength range from 400 to 2000 nm," *J. Phys. D: Appl. Phys.*, Vol. 38, No. 15, pp. 2543–2555, 2005.
18. M.J.C. Van Gemert, S.L. Jacques, H.J.C.M. Sterenborg et al., "Skin optics," *IEEE Trans. Biomed. Eng.*, Vol. 36, No. 12, pp. 1146–1154, 1989.
19. M. Straub, P. Lodemann, P. Holroyd et al., "Live cell imaging by multifocal multiphoton microscopy," *Eur. J. Cell Biol.*, Vol. 79, No. 10, pp. 726–734, 2000.
20. F. Stracke, B. Weiss, C.M. Lehr et al., "Multiphoton microscopy for the investigation of dermal penetration of nanoparticle-borne drugs," *J. Invest. Dermatol.*, Vol. 126, No. 10, pp. 2224–2233, 2006.
21. M.D. Cahalan and I. Parker, "Choreography of cell motility and interaction dynamics imaged by two-photon microscopy in lymphoid organs," *Annu. Rev. Immunol.*, pp. 585–626, 2008.
22. C.L. Phillips, L.J. Arend, A.J. Filson et al., "Three-dimensional imaging of embryonic mouse kidney by two-photon microscopy," *Am. J. Pathol.*, Vol. 158, No. 1, pp. 49–55, 2001.
23. G. Duemani Reddy, K. Kelleher, R. Fink et al., "Three-dimensional random access multiphoton microscopy for functional imaging of neuronal activity," *Nat. Neurosci.*, Vol. 11, No. 6, pp. 713–720, 2008.
24. J.J.G.H.M. Bergman and G.N.J. Tytgat, "New developments in the endoscopic surveillance of Barrett's oesophagus," *Gut*, Vol. 54, No. Suppl. 1, 2005.
25. G. Cinalli, P. Cappabianca, R. de Falco et al., "Current state and future development of intracranial neuroendoscopic surgery," *Expert Rev. Med. Devices*, Vol. 2, No. 3, pp. 351–373, 2005.
26. A.F. Low, G.J. Tearney, B.E. Bouma et al., "Technology insight: Optical coherence tomography—Current status and future development," *Nat. Clin. Pract. Cardiovasc. Med.*, Vol. 3, No. 3, pp. 154–162, 2006.
27. K. Sokolov, J. Aaron, B. Hsu et al., "Optical systems for in vivo molecular imaging of cancer," *Technol. Cancer Res. Treat.*, Vol. 2, No. 6, pp. 491–504, 2003.
28. W. Drexler and J. Fujimoto, *Optical Coherence Tomography: Technology and Applications*, Springer, New York, 2008.
29. A.P. Dhawan, "Early detection of cutaneous malignant melanoma by three-dimensional Nevoscopy," *Comput. Methods Prog. Biomed.*, Vol. 21, pp. 59–68, 1985.
30. V. Terushkin, S.W. Dusza, N.A. Mullani et al., "Transillumination as a means to differentiate melanocytic lesions based upon their vascularity," *Arch. Dermatol.*, Vol. 145, No. 9, pp. 1060–1062, 2009.
31. M.D. Max, "Cutler, "Transillumination of breasts," *J. Am. Med. Assoc.*, Vol. 93, No. 21, p. 1671, 1929.
32. D.R. Leff, O.J. Warren, L.C. Enfield et al., "Diffuse optical imaging of the healthy and diseased breast: A systematic review," *Breast Cancer Res. Treat.*, Vol. 108, No. 1, pp. 9–22, 2008.
33. L.S. Fournier, D. Vanel, A. Athanasiou et al., "Dynamic optical breast imaging: A novel technique to detect and characterize tumor vessels," *Eur. J. Radiol.*, Vol. 69, No. 1, pp. 43–49, 2009.
34. M.K. Simick and L.D. Lilge, "Optical transillumination spectroscopy to quantify parenchymal tissue density: An indicator for breast cancer risk," *British J. Radiology*, Vol. 78, pp. 1009–1017, 2005.
35. J.J. Niederhauser, *Real-Time Biomedical Optoacoustic Imaging*, Swiss Federal Institute of Technology, Zürich, Switzerland, 2004.
36. L.V. Wang, "Tutorial on photoacoustic microscopy and computed tomography," *IEEE J. Sel. Top. Quantum Electron.*, Vol. 14, No. 1, pp. 171–179, 2008.
37. H.F. Zhang, K. Maslov, G. Stoica et al., "Functional photoacoustic microscopy for high-resolution and noninvasive in vivo imaging," *Nat. Biotechnol.*, Vol. 24, No. 7, pp. 848–851, 2006.
38. G. Ku, B.D. Fornage, X. Jin et al., "Thermoacoustic and photoacoustic tomography of thick biological tissues toward breast imaging," *Technol. Cancer Res. Treat.*, Vol. 4, No. 5, pp. 559–565, 2005.
39. G. Ku and L.V. Wang, "Deeply penetrating photoacoustic tomography in biological tissues enhanced with an optical contrast agent," *Opt. Lett.*, Vol. 30, No. 5, pp. 507–509, 2005.

40. X. Wang, Y. Pang, G. Ku, X. Xie, G. Stoica, and L.V. Wang, "Noninvasive laser-induced photoacoustic tomography for structural and functional *in vivo* imaging of the brain," *Nature Biotechnology*, Vol. 21, pp. 803–806, 2003.
41. S. Dippel, M. Stahl, R. Wiemker, and T. Blaffert, "Multiscale contrast enhancement for radiographies: Laplacian pyramid versus fast wavelet transform," *IEEE Trans. Med. Imaging*, Vol. 21, pp. 343–353, 2002.
42. G. Cincoti, G. Loi, and M. Pappalardo, "Frequency decomposition and compounding of ultrasound medical images with wavelet packets," *IEEE Trans. Med. Imaging*, Vol. 20, pp. 764–771, 2001.
43. X. Hao, C.J. Bruce, C. Pislaru, and J.F. Greenleaf, "Segmenting high-frequency intercardiac ultrasound images of myocardium into infarcted, ischemic and normal regions," *IEEE Trans. Med. Imaging*, Vol. 20, pp. 1373–1383, 2001.
44. M. Moriyama, Y. Sato, H. Naito, M. Hanayama, T. Ueguchi, T. Harada, F. Yoshimoto, and S. Tamura, "Reconstruction of time-varying 3-D left ventricular shape multiview X-ray cineangiocardiograms," *IEEE Trans. Med. Imaging*, Vol. 21, pp. 773–785, 2002.
45. H.K. Huang, *PACS and Imaging Informatics: Principles and Applications*, John Wiley & Sons, Hoboken, NJ, 2004.
46. Z. Zhou, M.A. Gutierrez, J. Documet, L. Chan, H.K. Huang, and B.J. Liu, "The role of a data grid in worldwide imaging-based clinical trials," *J. High Speed Netw.*, Vol. 16, pp. 1–13, 2006.
47. M.Y.Y. Law, "A Model of DICOM-based electronic patient record in radiation therapy," *J. Comput. Med. Imaging Graph.*, Vol. 29, No. 2–3, pp. 125–136, 2006.